Indonesian Journal of Pharmacy

VOL 34 (1) 2023: 140–152 | RESEARCH ARTICLE

Co-Crystallization of Sofosbuvir with Sugars for Enhanced Dissolution Rate

Taher M. Mousa[1], Ahmed A. Donia[1], Gamal M. El Maghraby[2]

1. Department of Pharmaceutical Technology, Faculty of Pharmacy, Menofia University, Shebine El-kom, 11, Haron, Dokki, Giza, Egypt
2. Department of Pharmaceutical Technology, Faculty of Pharmacy, Tanta University, Tanta, Gharbia Governorate 6624033, Egypt

Article Info

Submitted: 30-08-2022
Revised: 10-12-2022
Accepted: 01-02-2023

*Corresponding author
Taher M. Mousa

Email:
taher.yassen@phrm.menofia.edu.eg

ABSTRACT

Sofosbuvir is one of the direct acting antiviral agents which is approved in the treatment of chronic hepatitis C virus (HCV) in combination with other agents. The low aqueous solubility of sofosbuvir resulted in slow dissolution which is supposed to be responsible for its low and variable bioavailability after oral administration. Accordingly, the objective of this work was to investigate the effect of co-crystallization of sofosbuvir with hydrophilic sugars such as sucralose, xylitol or mannitol on its crystalline structure and dissolution rate. Mixtures of sofosbuvir with hydrophilic sugars at various molar ratios (1:1 and 1:2) were prepared by ethanol assisted kneading followed by drying. The dry products were then characterized by attenuated total reflectance Fourier transform infrared spectroscopy (ATR FTIR), differential scanning calorimetry (DSC), powder X-ray diffraction (XRD) and in vitro dissolution studies. Combined instrumental analysis reflected development of new crystalline species of co-crystal type. This was evidenced by the existence of hydrogen bonding as shown from FTIR spectra, change in the thermal behaviour and appearance of new diffraction peaks in the diffractograms recorded by XRD. The co-crystallization was associated by weakening of intermolecular bonds which resulted in significant increase ($P < 0.05$) in the dissolution rate of sofosbuvir. The study introduced hydrophilic sugars as co-crystal co-formers for enhanced dissolution of sofosbuvir.

Keywords: Sofosbuvir co-crystals, Hydrophilic sugars, Wet co-grinding method, Dissolution efficiency; Powder X-ray diffraction pattern.

INTRODUCTION

Treatment of hepatitis-C virus (HCV) has been advanced after development of orally active direct-acting antiviral agents (DAAs) (Charlton *et al.,* 2015). Sofosbuvir is one of the direct acting antiviral agents which is approved in the treatment of chronic HCV in combination with other agents. It acts via blocking of the RNA polymerase which subsequently inhibits RNA replication of HCV (Berden *et al*., 2014). Sofosbuvir is a crystalline solid, slightly soluble in water and its water solubility nearly 2 mg/mL with a pH independent solubility across pH range of 2 to 7.7 (Tucker, 2013; Chakravarthy *et al.,* 2016). The low aqueous solubility of sofosbuvir resulted in slow dissolution which is believed to be responsible for its low and variable bioavailability (9% in dogs as reported in European Medicine Agency, 2016) after oral administration. Accordingly, rapid dissolution is estimated to improve its bioavailability and therapeutic efficacy.

Various techniques are useful for improved dissolution rate of poorly aqueous soluble drugs. Examples of these strategies include reduction in particle size via milling or controlled crystallization (Ochi *et al.,* 2014; Khadka *et al.,* 2014; Dizaj *et al*., 2015; Choi & Park 2017; Sironi *et al.,* 2017), salt formation (Ochi *et al.,* 2013) micro and nano emulsion formation (Hu *et al*., 2011; Kang *et al.,* 2012; Reis *et al.,* 2013; Xing *et al.,* 2016), solid dispersions (Moretti *et al.,* 2001; Ziaee *et al.,* 2017) and formation of inclusion complex with cyclodextrins (Rawat & Jain 2004; Bouchal *et al.,* 2015; Samprasit *et al*., 2018).

Copyright © 2023 by Indonesian Journal of Pharmacy (IJP). The open access articles are distributed under the terms and conditions of Creative Commons Attribution 2.0 Generic License (https://creativecommons.org/licenses/by/2.0/).

Table I. The compositions of the tested formulations presented as molar and weight ratio for Sofosbuvir.

	Molar ratio	**Weight ratio**			
		Sofosbuvir (mg)	Sucralose (mg)	Xylitol (mg)	Mannitol (mg)
Sofosbuvir	-	400	-	-	-
F1	1:1	400	300.44	-	-
F2	1:2	400	600.89		
F3	1:1	400	-	114.96	-
F4	1:2	400	-	228.92	-
F5	2:1	400	-	-	68.82
F6	1:1	400	-	-	137.64
F7	1:2	400	-	-	275.28

Co-crystallization has been emerged as promising strategy for enhanced dissolution rate with encouraging data being recorded (Chun *et al.,* 2013; Arafa *et al.,* 2016, 2018; Essa *et al.,* 2019).

Pharmaceutical cocrystal is a stoichiometric multi-component system of the given drug with benign co-former. Co-crystallization takes place with non-covalent interactions developing solid product which undergoes fast dissolution while preserving the original pharmacological activity (Jones *et al.*, 2006; Arafa *et al*., 2016). Unlike salt formation, which is achieved between ionizable materials, co-crystallization can be achieved even in absence of ionizable compounds. (Velaga *et al.,* 2008; Apshingekar *et al*., 2017; Cysewski & Przybyłek, 2017). In addition, co-crystals are more stable than metastable polymorphs, amorphous drug or solid dispersions (Viertelhaus & Hafner, 2015).The major advantage of co-crystallization is based on the ease of fabrication with alternative techniques being available for use. Co-crystals can be prepared by dry or liquid assisted grinding (He *et al*., 2008; Arafa *et al.,* 2016, 2018), supercritical fluid (Padrela *et al*., 2010) or hotmelt extrusion (Boksa *et al.,* 2014). Various co-formers have been employed for co-crystal formation with the developed co-crystals showing hastened dissolution. According to Arafa *et al.,* (2016) the dissolution rate of hydrochlorothiazide cocrystals prepared with sucralose was higher than that of pure hydrochlorothiazide. The dissolution rate of felodipine cocrystals prepared with xylitol was higher than that of pure felodipine (Arafa *et al.*, 2018). Bicalutamide showed magnified dissolution rate after co-crystallization with sucralose (Essa *et al.*, 2019). The dissolution rate of glimepiride was also improved by co-crystallization with water-soluble co-formers such as citric acid, tartaric acid and oxalic acid dihydrate (Jaafar & Radhi, 2020). A patent is available on sofosbuvir co-crystal with amino acids (WO 2016/042576 A1). Development of co-crystals with commonly used excipients will add advantages. Accordingly, the objective of this work was to investigate the effect of co-crystallization of sofosbuvir with hydrophilic sugars on the dissolution rate of the drug.

MATERIALS AND METHODS

Crystalline Sofosbuvir (98% purity), sucralose and mannitol were donated by AUG pharma, 6- October City, Giza, Egypt. Xylitol was obtained from Sigma Pharmaceutical Industries, Quesna, Egypt. Potassium dihydrogen phosphate, dipotassium hydrogen phosphate, Tween 80 and ethanol (pharmaceutical grade) were obtained from El Nasr Pharmaceutical Chemicals Company, Cairo, Egypt.

Preparation of co-processed mixtures

Co-processing involved simultaneous kneading which involved mixing of sofosbuvir with the required amount of additive in the mortar (Table I). Ethanol was added gradually with mixing to form smooth paste. Mixing continued to develop dry flowing mixture. This process was repeated 4 times and the product was stored in an air-tight container (Kassem *et al.*, 2021).

FTIR Spectroscopy

The FTIR spectra of the unprocessed and processed materials were collected using ATR FTIR spectrophotometer of FT/IR-4100type A (Jasco, Japan). This equipment is supported by a TGS detector with data acquisition and analysis being achieved using Jasco spectra manager version 2 Software. The dry powdered samples were loaded into the specified holder and scanning from 4000 to 400 cm^{-1} with resolution of 4 cm^{-1}.

Differential Scanning Calorimetry (DSC)

Thermal analysis studies utilized a differential scanning calorimeter (TA DSC25, New Castle, USA). Known weight (about 3mg) of the sample was packed into aluminum pan which was crimped after mounting the lid. The sample pan was loaded into the sample holder with crimped empty pan being utilized as reference. Data acquisition was performed while heating the sample at a heating rate of 10°C /minute, starting from 30°C and ending at 400°C. Data acquisition and analysis were conducted using TRIOS software.

Powder X-ray diffraction (PXRD)

XRD patterns of selected samples were obtained using an X-Ray diffractometer (XRD Bruker CO D8 advance, Germany) equipped with a Cu radiation source (1.54° A) operating at 40 mA and 40 kV. Data was recorded from 2θ angle of 3° to 60° at a step size of 0.03°.

Spectrophotometric determination of Sofosbuvir

Sofosbuvir was quantified using UV spectrophotometry at wavelength of 260 nm. An accurately weighed amount (50 mg) of sofosbuvir was dissolved in 10 mL methanol in a volumetric flask to prepare 5000 µg/mL (stock I). This solution was diluted 1 in 100 with 0.15 % Tween 80 in 10 mM potassium phosphate buffer (pH 6) to prepare 50 µg/mL (stock II). The working stock was used to prepare series of concentrations in the range of 5 to 50 µg/mL using 0.15 % tween 80 in 10mM potassium phosphate buffer (pH 6). The absorbance of each solution was measured at 260 nm against a suitable blank. Each experiment was carried out in triplicate and the average absorbance was plotted against the concentration to construct the calibration curve.

The method was validated for quantification of sofosbuvir. The validation was conducted according to the ICH guidelines. The validation parameters included linearity which was determined from the correlation coefficient recorded after linear regression analysis of the standard calibration curve. The validation parameters included determination of the linearity range which was taken as the range between the lowest and highest concentration in the calibration curve. The accuracy is estimated by comparing the nominal values to the recorded values of 5 concentrations selected from the calibration curve and subjected to replicate analysis in the same day and in different days. The results of intraday and inter-day replicate analysis were adopted to calculate the relative standard deviation (RSD) which was used as a measure for the intra and inter-day precision. The lower limit of detection (LOD) and lower limit of quantification (LOQ) were computed using the following equations.

LOD = 3.3 x (SD intercept / S)

Where, SD is the standard deviation of the intercept and S is the slope of the corresponding calibration curve.

LOQ = 10 x (SD intercept / S)

Where, SD is the standard deviation of the intercept and S is the slope of the corresponding calibration curve

Saturation Solubility studies

The solubility of pure sofosbuvir and the co-processed mixtures was determined in distilled water at ambient temperature. Excess solids were added to screw-capped glass test tubes containing 10 mL distilled water. This was mixed continuously in Memmert shaker water bath (GmbH, Germany) for 72 h at the end of which the samples were filtered through a 0.45 µm Millipore filter. The concentration of drug in the filtrate was determined by UV spectrophotometry at 260 nm. Three replicates were conducted for each sample.

Dissolution Studies

The dissolution behaviors of sofosbuvir was monitored before and after co-processing with selected hydrophilic excipients. The studies were conducted using USP II (paddle type) Dis 6000 dissolution apparatus which was made by Copley Scientific, Nottingham, UK. Sink conditions were maintained by 900 mL of dissolution medium composed of 1.5 % w/v Tween 80 in potassium phosphate buffer (10 mM, pH 6) which was maintained at 37 ± 1°C throughout the experiment. This dissolution medium was chosen according to FDA dissolution methods for sofosbuvir. The equipment was adjusted so as to rotate the paddle at 75 rpm. 400 mg of pure sofosbuvir and powdered samples equivalent to 400 mg of sofosbuvir were introduced into the dissolution vessels. Samples (5 mL) were collected at selected time intervals (5, 10, 15, 20, 30, 45, and 60 minutes). The dissolution samples were instantaneously filtered through a 0.45 µm Millipore filter and the dissolution volume was replenished with equivalent volume of fresh medium. The concentration of drug in each sample was quantified using the developed spectroscopic method of analysis. The cumulative amounts of drug liberated were calculated as percentage of the dose and were plotted as a function of time to

obtain the dissolution profiles. The percentage of drug dissolved in the first 5 minutes was computed as Q5. The dissolution efficiency (DE %) was also computed according to the established procedures (Khan, 1975). The mean dissolution time (MDT) was calculated according to the equation described by Costa and Sousa Lobo, (2001). Q5, MDT and DE% were used to statistically compare between formulations. Statistical treatment also employed the similarity factor test which was computed using the following equation.

$$F_s = 50 \text{ X } \log \{[1+ (\frac{1}{n}) \sum_{t=1}^{n}(R_t - T_t)^2]^{-0.5} \text{ X}100\}$$

Where n is the number of data points, (R_t) is the amount of the reference dissolved (%) at time t and (T_t) is the amount of the test dissolved (%) at the same time. F_s value higher than 50 and close to 100 show the similarity of the dissolution profiles.

Statistical Analysis

In addition to similarity factor test, dissolution parameters of the co-processed mixtures were compared to unprocessed sofosbuvir using Kruskal-Wallis test with Tukey's multiple comparison as post hoc. This was done using IBM SPSS statistics 20 software.

RESULTS AND DISCUSSION

FTIR spectroscopy

FTIR spectroscopy was utilized to monitor any interaction between the active pharmaceutical ingredient and the tested coformers. This was achieved by monitoring the position and width of the principle absorption bands before and after co-processing (Sopyan *et al.*, 2017). Figure 1 shows the FTIR spectra of sofosbuvir before and after co-processing with sucralose, xylitol and mannitol. The FTIR spectrum of pure unprocessed sofosbuvir shows the absorption bands correlating with its functional groups. These included the absorption bands at 3251 cm^{-1} for NH stretching vibrations, at 3342 cm^{-1} for alcoholic OH, at 3089 cm^{-1} for CH stretching, at 2980 cm^{-1} for CH_3 stretching, at 1719 cm^{-1} and 1669 cm^{-1} for the ester and amide C=O stretching vibrations, at 1595 cm^{-1} for C=C stretching vibrations, an absorption band at 1455 cm^{-1} for CH_2CH_3 bending vibration. The P=O bending vibration was seen at 1265 cm^{-1} and CO bending vibration was recorded at 1091 cm^{-1}. The NH wagging was shown at 945.9 cm^{-1}. This spectrum highlights the chemical structure of sofosbuvir and agrees with the published spectrum (Lankalapalli *et al.,* 2017; Mehmood *et al.,* 2020; Islam *et al.,* 2021).

The FTIR spectrum sucralose revealed an absorption bands at 3455.8 and 3314 cm^{-1} for free and bonded OH-stretching, at 1300.7 cm^{-1}, 1119cm^{-1} , 1091 cm^{-1}, 1000.8 cm^{-1} and 889.9 cm^{-1} for C-O stretching and at 774 cm^{-1}, 663 cm^{-1} and 619 cm^{-1} for C-Cl. This spectrum is similar to published data on the same sugar (Brizuela *et al.,* 2013; Arafa *et al*., 2016, 2017; Essa *et al.,* 2019).

Wet co-grinding of sofosbuvir with sucralose produced powdered formulation with FTIR spectrum showing overlapping of the NH stretching of sofosbuvir and the OH of sucralose which made it difficult to monitor the changes in the absorption band of NH stretching. The only noticeable change was seen in the absorption band of NH wagging which showed shifting to 943 cm^{-1} with broadening (Figure 1). This change reflects possible hydrogen bonding. Broadening and shifting to lower wave number was assigned for hydrogen bonding (Arafa *et al*., 2016, 2017).

The FTIR spectrum of xylitol revealed absorption bands at 3420 cm^{-1}, 3357.4 cm^{-1} and 3289.9 cm^{-1} for free and bonded OH stretching, at 2991 cm^{-1} for C-H stretching, at 1471.4 cm^{-1} for C-H bending. The C-O stretching was shown at 1087.6 cm^{-1}, 1062.5 cm^{-1} and 1004.7 cm^{-1}. This spectrum is similar to that recorded in other investigations (Arafa *et al.,* 2018).

Wet co-grinding of sofosbuvir with xylitol resulted in alterations in the absorption bands corresponding to the NH stretching vibrations and wagging. These changes were reflected as broadening and shifting to lower wave number suggesting hydrogen bonding (Figure 1).

The FTIR spectrum of mannitol showed characteristic absorption bands covering the range of 3450 to 3050 cm^{-1} presenting the free and bonded OH stretching vibrations (Figure 1). The C-O stretching was noticed at 1077 cm^{-1} and 1017.2 cm^{-1}. These spectral features correlate with that recorded in other studies (Rajbanshi *et al*., 2014; Pêcego, 2018).

Wet co-grinding of sofosbuvir with mannitol showed signs of hydrogen bonding which were revealed as broadening and shifting to lower wave numbers in the absorption bands corresponding to the NH stretching and wagging (Figursie 1). The interaction between NH group of sofosbuvir and OH group of sugar is responsible for hydrogen bond formation.

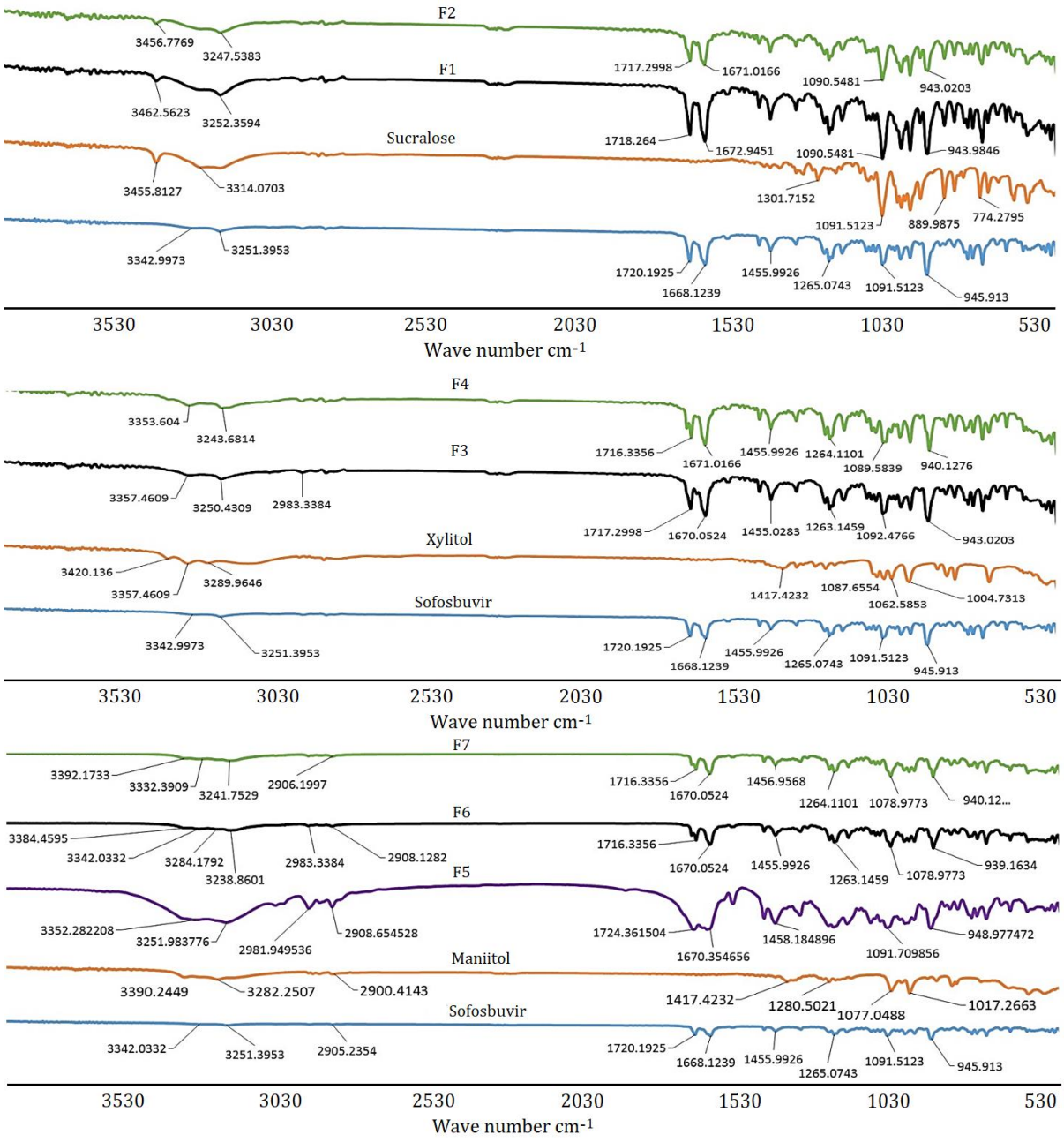

Figure 1: FTIR spectra of unprocessed sofosbuvir, sucralose, xylitol, mannitol and their co- processed mixtures in various molar ratios.

Differential Scanning Calorimetry

Thermal behavior of sofosbuvir, sucralose, xylitol, mannitol and the fabricated co-processed mixtures was studied with the help of DSC. The thermogram of pure unprocessed sofosbuvir showed its melting transition which were seen as endothermic peak with a T_m value of 133.82°C and an enthalpy of 40.69 J/g (Figure 2). This melting endotherm correlates with crystalline structure of sofosbuvir. The thermogram revealed also thermal decomposition event of sofosbuvir which was shown as broad exothermic peak with T_m value of 255°C (Figure 2). Similar thermal behavior was reported for sofosbuvir by other researchers who showed its melting transition at 129.17°C (Mehmood *et al*., 2020).

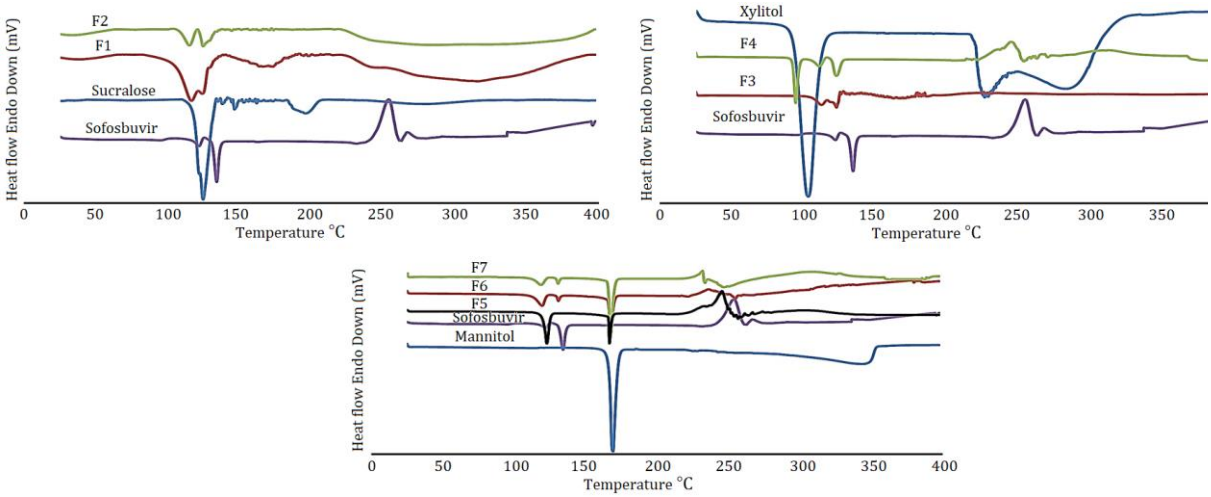

Figure 1. DSC thermogram of unprocessed sofosbuvir, sucralose, xylitol, mannitol and their co- processed mixtures in various molar ratios.

Table II. DSC thermograms of unprocessed sofosbuvir, sugars, and their co-processed formulations.

	Onset (°C)	**Endset (°C)**	**Tm (°C)**	**Enthalpy J/g**
Sofosbuvir	129.66, 238.53	139.03, 261.24	133.82, 244.88	40.69, 112.7
Sucralose	116.40	132.55	124.69	95.55
Xylitol	86.76	119.21	103.11	1881
Mannitol	158.86	176.88	169.22	230.9
F1	103.9	129.8	116.65	158.8
F2	108.1	119.83	115.28	31.15
F3	88.57, 118.13	99.39, 128.58	94.32, 122.6	60.6, 29.29
F4	88.21	100.46	94.16	102.68
F5	104.88, 152.31	129.32, 177.85	122.85, 166.75	73.99, 35.2
F6	103.42, 161.02	127.14, 172.92	119.58, 168.00	51.92, 50.69
F7	104.52, 162.83	126.41, 174	118.92, 167.70	42.39, 144.32

The thermal behavior of sucralose was characterized by sharp endotherm with T_m of 124.69°C and enthalpy of 95.55 J/g. This correlates with the published data on the sugar (Brizuela *et al.,* 2013; Arafa *et al*., 2016, 2017; Essa *et al.,* 2019).

Co-processing of sofosbuvir with sucralose produced a mixture with thermal behavior different from the thermal pattern of both materials. The thermogram of the co-processed mixture was characterized by biforked endotherm transition with Tm values at 116.8 and 124.3°C. The biforked endotherm was isolated as two endothermic peaks in mixtures containing sofosbuvir and sucralose at 1:2 molar ratios. This pattern suggests transformation of the crystalline structure of both materials to new crystalline species. Interestingly, the exothermic decomposition of sofosbuvir was not recorded in the co-processed mixtures (Figure 2 and Table II). Taking the recorded changes in the thermal behavior with the noticed alterations in the FTIR spectra, the developed crystalline species may be of co-crystalline type (to be confirmed by X-ray diffraction in the proceeding section). Development of co-crystals with lower melting point indicates weakening of intermolecular bonding which can subsequently hasten the dissolution rate. Sucralose has been shown to develop co-crystalline products with other drugs (Arafa *et al.*, 2016, 2017; Essa *et al*., 2019).

The thermogram of pure xylitol showed a sharp endothermic peak with Tm of 103.11°C and enthalpy of 1881 J/g. This endotherm represents the melting transition of the sugar correlating with the published data on the sugar (Arafa *et al*., 2018).

For sofosbuvir-xylitol co-processed mixtures (1:1 molar ratio), the main endothermic peak of the drug was shown at lower Tm values (122°C) compared with the unprocessed drug. This was associated with disappearance of the endothermic peak of xylitol. Further increase in xylitol produced similar endothermic peak at 122°C with an endotherm corresponding to excess xylitol appearing at 94.3°C (Figure 2 and Table II). Interestingly, the exothermic decomposition of sofosbuvir was not recorded in the co-processed mixtures. The recorded changes in the thermogram after wet co-grinding with xylitol can be attributed to possible co-crystal formation. This supposition is supported by the recorded evidence for hydrogen bonding in the FTIR spectral analysis. The potential of xylitol to form cocrystals with active pharmaceutical ingredients has been shown in literature (Arafa *et al.,* 2018).

The thermogram of pure mannitol showed characteristic sharp endotherm of its melting transition at 169.22°C (Figure 2). This behavior simulates that published for mannitol by other researchers who showed its melting transition at 168.4 and 167°C (Jaipal *et al*., 2014; Pêcego, 2018). Coprocessing of sofosbuvir with mannitol produced crystalline materials with compromised thermogram depending on the relative mole fraction. Formulation containing the drug with mannitol at 2:1 molar ratio produced two sharp endotherms, the first of which was noticed at 122.7 °C and the second was recorded at 166.7°C. Further increase in mannitol produced broadening of the first endotherm. The exothermic transition of the decomposition of sofosbuvir underwent progressive reduction in the Tm with increasing mannitol concentration (Figure 2 and Table II). These changes suggest possible changes in the crystalline structure which may be due to development of co-crystalline product which is supported by the FTIR spectroscopic changes.

Powder X-ray diffraction pattern (PXRD)

The PXRD of sofosbuvir, sucralose, xylitol, mannitol and the co-processed mixtures are shown in Figure 3. The recorded diffraction peaks are presented in Table III. The diffractogram of the unprocessed sofosbuvir showed the characteristic diffraction pattern of sofosbuvir crystals with strong diffraction peaks being noticed (Figure 3 and Table III). This diffractogram coincides with that recorded for sofosbuvir in other studies (Mehmood *et al*. 2020). The crystalline characteristics for sucralose, xylitol, mannitol were also demonstrated in the diffractograms as reflected from the recorded intense diffraction peaks (Figure 3 and Table III). Co-processing of sofosbuvir with sucralose produced new crystalline species an X-ray diffraction pattern different from both the individual components. The difference was shown as broadening of peaks and appearance of new diffraction peaks at 2 θ values of 13.665°, 14.025°, 17.678°, 23.021°, 30.156°, 36.387°, 37.98° and 39.307°. This supports the thermal behavior and confirms the development of co-crystalline product (Arafa *et al.,* 2016).

Co-processing of sofosbuvir with xylitol produced crystalline mixture with compromised diffractogram compared to that of the starting components. The compromise was shown as broadening of the diffraction peaks and appearance of new peaks at 2θ values of 19.768°, 20.780°, 22.501°, 24.616°, 27.671°, 30.092°, 31.479°, 33.818°, 35.38° and 42.402° and 44.275° (Figure 3 and Table III). These changes support development of new crystal phase (co-crystal) and confirms the suitability of xylitol as co-crystal co-former (Arafa *et al.,* 2018).

For sofosbuvir-mannitol co-processed mixture, the PXRD pattern was different from the simple pattern of both the unprocessed sofosbuvir and mannitol. The difference was reflected by appearance of new diffraction peaks. The new peaks were recorded at 2θ values of 14.621°, 23.388°, 29.455°, 30.051°, 31.349°, 33.591°, 38.718° and 44.09° (Figure 3 and Table III). Development of new diffraction peaks confirms the transformation to new crystalline species and augment the findings of DSC and FTIR. This behavior supports the formation of co-crystalline product. Similar conclusion was presented by in other studies after recording similar changes in the combined instrumental data recorded after co-processing of drugs with co-crystal co-formers (Bak *et al*., 2008; Wang *et al.,* 2013; Arafa *et al*., 2016, 2018; Essa *et al.,* 2019).

Spectrophotometric determination of sofosbuvir

Calibration curve of sofosbuvir constructed and showed good linearity within the concentration range of 5 to 50 µg/mL with equation of Y=0.0176X-0.043 and correlation coefficient of 0.9994. The mean percentage of recovery for the studied concentrations was 99.80% of the nominal values. The lower limit of detection was calculated to be 0.868 µg/mL and the lower limit of quantitation was 2.63 µg/mL.

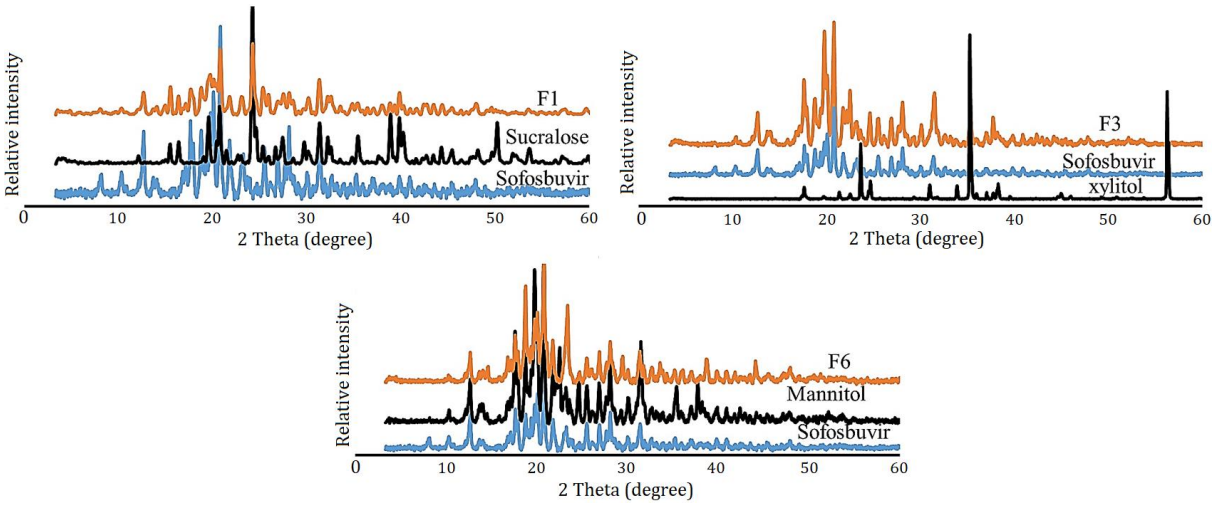

Figure 3. X- ray diffraction pattern of unprocessed sofosbuvir, sucralose, F1, xylitol, F3, mannitol and F6.

Table III. Powder x-ray diffraction pattern of unprocessed sofosbuvir, sugars and their co-processed formulations

	2θ angle
Sofosbuvir	8.148, 10.316, 12.651, 17.126, 17.729, 18.771, 19.389, 19.776, 20.078, 20.8, 21.777, 25.514, 26.899, 27.655, 28.091, 31.39, 32.633, 35.223, 37.057, 40.921°.
Sucralose	15.446, 16.382, 19.557, 20.699, 24.205, 24.6 25.312, 25.919, 26.653, 29.703 31.346, 32.208, 35.367, 37.67, 38.854, 39.807, 40.21, 50.182 °.
Xylitol	17.613, 23.633, 24.686, 30.985, 33.895, 35.256, 38.274, 56.332°.
Mannitol	12.650, 17.60, 17.90, 18.759, 19.753, 20.06, 20.778, 21.77, 22.509, 23.114, 23.595, 24.635, 25.517, 26.866, 27.656, 28.086, 30.07, 31.475, 35.392, 37.017, 37.733, 38.19 °.
F1	12.665, 15.517, 16.406, 17.138, 17.678, 18.829, 19.667, 20.791, 21.778, 23.021, 24.239, 25.302, 25.887, 27.461, 28.114, 31.293, 32.207, 32.541, 34.837, 35.367, 36.387, 37.037, 37.980, 38.817, 39.307, 39.805, 40.280, 40.919, 42.486, 42.696, 43.418 °.
F3	12.653, 17.605, 18.742, 19.768, 20.062, 20.780, 21.834, 22.501, 23.205, 23.571, 24.616, 25.490, 26.896, 27.671, 28.092, 28.574, 30.092, 31.479, 35.380, 37.739, 38.183, 39.838, 40.901 °.
F6	12.663 ,14.621, 16.883, 17.161, 17.626, 17.891, 18.753, 19.768, 20.065, 20.791, 21.761, 23.388, 25.518, 25.956, 26.896, 27.757, 28.087, 29.455, 30.051, 31.349, 31.760, 32.673, 33.591, 38.718, 44.099 °.

The accuracy of the assay was evaluated and the percentage recovery for studied concentrations was in the range of 98.61 to 101.97 % of the nominal values (optimum ± 2%). The precision of the assay was evaluated for both inter and intra-day. The RSD was in the range of 0.74 to 3.89 % for intra-day and was in the range of 0.84 to 1.8 % for inter-day results.

Saturation Solubility studies

The solubility of sofosbuvir was increased after co-crystallization with hydrophilic sugars (Table IV). The magnitude of increase depended on the type of sugar with sucralose being the most effective. Similar findings concerning solubility enhancement were reported with cocrystals of piroxicam, meloxicam, niclosamide and fluoxetine hydrochloride (Childs *et al*., 2004; Cheney *et al*., 2011; Sanpuhi *et al*., 2012; Panzade *et al*., 2017).

Dissolution Studies

The dissolution behavior of pure unprocessed sofosbuvir was erratic with only 28.98 % of the dose dissolving in the first 5 min (Q5). Slow dissolution continued to liberate 75.72% at the end of experiment (60 minutes).

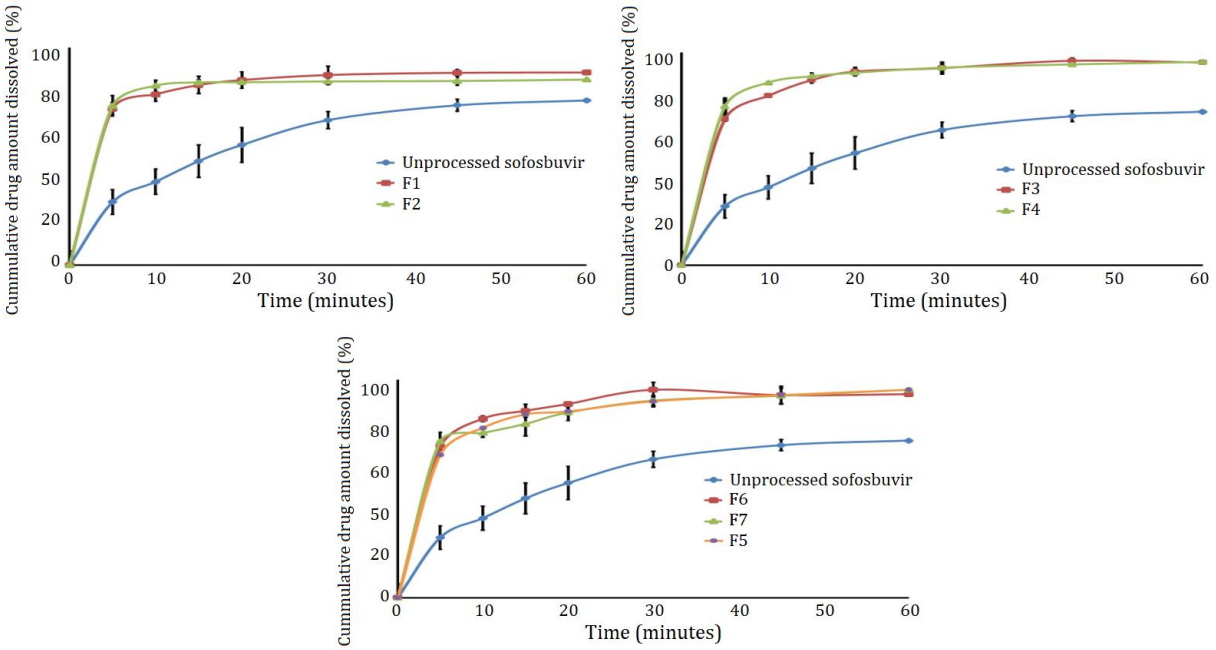

Figure 4: Dissolution profile of unprocessed sofosbuvir, F1, F2, F3, F4, F5, F6 and F7.

Table IV: The dissolution Efficiency (DE), Q5, MDT, solubility and similarity factor (Fs) values of sofosbuvir and the prepared formulations.

	Q5 (%)	MDT (min)	DE (%)	Solubility (mg/mL)	Fs
Sofosbuvir	28.98 (6.547)	13.9 (0.875)	58.23 (5.34)	2.88 (0.617)	-
F1	71.95 (5.27)	5.371 (0.222)	81.46 (3.385)	6.02 (0.654)	29.8
F2	73.21 (5.364)	4.444 (0.885)	79.9 (0.728)	6.322 (0.94)	29.5
F3	72.07 (0.516)	4.93 (0.18)	90.81 (0.1321)	3.5 (1.18)	25.19
F4	78.33 (6.368)	4.26 (0.926)	91.28 (0.201)	4.675 (0.376)	24
F5	68.92 (0.189)	6.16 (0.03)	87.79 (1.02)	3.357 (0.514)	27.03
F6	72.87 (2.748)	5.58 (0.213)	89.95 (1.48)	3.44 (0.947)	25.38
F7	75.33 (1.288)	5.303 (0.203)	87.66 (3.125)	3.55 (0.914)	27.08

Q5 (%) is the amount dissolved at 5 min and DE (%) is the dissolution efficiency.MDT is the mean dissolution time (minutes), Fs is similarity factor. Values between brackets represent standard deviation values (S.D.), n = 3.

The overall dissolution efficiency and the mean dissolution time (MDT) were 58.23% and 13.9 minutes respectively (Figure 4 and Table IV). The recorded slow dissolution complies with the published work on unprocessed sofosbuvir which required 4 hour to reach 100% dissolution with less than 60% dissolving in the first hour (Mehmood *et al.,* 2020). Co-processing of sofosbuvir with sucralose resulted in significant increase in the dissolution rate and the dissolution efficiency. The significance was indicated by comparing the dissolution parameters of the tested formulations with that of the unprocessed sofosbuvir ($P < 0.05$). The recorded Q5 values were 71.95% and 73.21% for formulations F1 and F2, respectively. In addition, the total amounts of sofosbuvir dissolved in 60 min were 88.59 % and 85.30 % for formulations F1 and F2, respectively. The computed dissolution efficiency value of sofosbuvir after 60 min were 81.46 % and 79.9 % for the same formulations, respectively (Figure 4 and Table IV). It was also noticed that the dissolved amount of sofosbuvir in formulations F1 and F2 after five minutes was increased (2.5-fold) as compared to pure drug. The mean dissolution time was 5.37 and 4.44 minutes for formulations F1 and

F2, respectively. The increase in the overall dissolution of sofosbuvir was further confirmed by the similarity factor test which was performed on the dissolution data of each formulation compared with that of unprocessed sofosbuvir. The computed similarity factor (Fs) values for formulations F1 and F2 was 29.8 and 29.5 % respectively. It worth noting that no significant difference was recorded between the sofosbuvir dissolution from formulations F1 and F2 (Fs > 50%). The enhanced dissolution rate can be explained on the base of co-crystallization between sofosbuvir and sucralose. The insertion of the hydrophilic sucralose molecule within the crystal lattice of sofosbuvir developed co-crystals with weakened intermolecular bonds. This can subsequently hasten the dissolution rate. Enhancement of dissolution behavior of hydrophobic drugs has been shown after co-crystallization with sucralose (Arafa *et al*., 2016, 2017; Essa *et al*., 2019).

As for sucralose, co-processing of sofosbuvir with xylitol resulted in significant increase in the dissolution rate of sofosbuvir irrespective to the molar ratio of xylitol to drug. The significance was indicated by comparing the dissolution parameters of the tested formulations with that of the unprocessed sofosbuvir ($P < 0.05$). The amount of the drug dissolved in the first 5 minutes was 72.07% and 78.33% in formulation F3 and F4 respectively. The rest of the dose was almost liberated after 15 minutes (Figure 4 and Table IV). The computed dissolution efficiency values after 60 minutes were 90.81 and 91.28 for the same formulations, respectively. The increase in the overall dissolution of sofosbuvir was further confirmed by the similarity factor test which reflected the superiority of the co-processed formulations (Fs < 50%). The mean dissolution time was 4.93 and 4.26 minutes for formulations F3 and F4, respectively. The amount dissolved of sofosbuvir after five minutes was increased 2.5 to 2.7 fold in cocrystal formulations F3 and F4 as compared to pure sofosbuvir. Similar release profiles were recorded for xylitol containing formulations (Table IV). This can be explained based on co-crystallization process which disrupted the intermolecular bonds. Similar behavior was shown for xylitol after co-crystallization with other drugs (Arafa *et al.,* 2018).

Co-processing of sofosbuvir with mannitol resulted in significant increase in the dissolution rate as shown from the computed dissolution parameters compared with the unprocessed sofosbuvir ($P<0.05$). This was evident irrespective to the amount of mannitol added in co-processing process. The Q5 values were 68.92, 72.87 and 75.33% for formulations F5, F6 and F7, respectively. The rest of the dose was subsequently liberated (Figure 4 and Table IV). The computed overall dissolution efficiency values were 87.79, 89.95 and 87.66% for the same formulations, respectively. The amount dissolved of sofosbuvr after five minutes was increased 2.5 to 2.7 fold in cocrystal formulations F5, F6 and F7 as compared to pure sofosbuvir. The superiority was confirmed from the computed similarity factor test (Table IV). The mean dissolution time was 6.16, 5.58 and 5.3 minutes for formulations F5, F6 and F7, respectively. The enhanced dissolution rate can be explained on the same base used to explain the recorded enhancement with xylitol and sucralose.

CONCLUSION

Ethanol assisted co-processing of sofosbuvir with mannitol, xylitol or sucralose produced new crystalline products exhibiting thermal and X-ray diffraction behavior different from those of the starting materials. The recorded instrumental data supported co-crystal formation. Co-crystallization with these sugars hastened the dissolution rate of sofosbuvir. The best formula was F4 as it has higher dissolution efficiency. The amount dissolved of sofosbuvir after five minutes in cocrysal formuations was increased 2.5 to 2.7 fold as compared to pure drug. The study thus introduced simple kneading as a tool for co-crystallization of sofosbuvir for augmented dissolution. The process may be performed during routine wet granulation process allowing easy scaling up but this requires verification.

ACKNOWLEDGEMENT

This research was supported by Tanta University and Menofia University.

REFERENCES

Apshingekar, P. P., Aher, S., Kelly, A. L., Brown, E. C., & Paradkar, A. (2017). Synthesis of caffeine/maleic acid co-crystal by ultrasound-assisted slurry co-crystallization. *Journal of pharmaceutical sciences*, *106*(1), 66-70.

Arafa, M. F., El-Gizawy, S. A., Osman, M. A., & El Maghraby, G. M. (2016). Sucralose as co-crystal co-former for hydrochlorothiazide: development of oral disintegrating

tablets. *Drug Development and Industrial Pharmacy*, *42*(8), 1225-1233..

Arafa, M. F., El-Gizawy, S. A., Osman, M. A., & El Maghraby, G. M. (2017). Co-crystallization for enhanced dissolution rate of nateglinide: In vitro and in vivo evaluation. *Journal of Drug Delivery Science and Technology*, *38*, 9-17.

Arafa, M. F., El-Gizawy, S. A., Osman, M. A., & El Maghraby, G. M. (2018). Xylitol as a potential co-crystal co-former for enhancing dissolution rate of felodipine: preparation and evaluation of sublingual tablets. *Pharmaceutical development and technology*, *23*(5), 454-463.

Bak, A., Gore, A., Yanez, E., Stanton, M., Tufekcic, S., Syed, R., ... & Koparkar, A. (2008). The co-crystal approach to improve the exposure of a water-insoluble compound: AMG 517 sorbic acid co-crystal characterization and pharmacokinetics. *Journal of pharmaceutical sciences*, *97*(9), 3942-3956.

Berden, F. A. C., Kievit, W., Baak, L. C., Bakker, C. M., Beuers, U., Boucher, C. A. B., ... & Drenth, J. P. H. (2014). Dutch guidance for the treatment of chronic hepatitis C virus infection in a new therapeutic era. *Netherlands Journal of Medicine*, *72*(8), 388-400.

Boksa, K., Otte, A., & Pinal, R. (2014). Matrix-assisted cocrystallization (MAC) simultaneous production and formulation of pharmaceutical cocrystals by hot-melt extrusion. *Journal of pharmaceutical sciences*, *103*(9), 2904-2910.

Bouchal, F., Skiba, M., Chaffai, N., Hallouard, F., Fatmi, S., & Lahiani-Skiba, M. (2015). Fast dissolving cyclodextrin complex of piroxicam in solid dispersion Part I: Influence of β-CD and HPβ-CD on the dissolution rate of piroxicam. *International Journal of Pharmaceutics*, *478*(2), 625-632.

Brizuela, A. B., Raschi, A. B., Castillo, M. V., Leyton, P., Romano, E., & Brandán, S. A. (2013). Theoretical structural and vibrational properties of the artificial sweetener sucralose. *Computational and Theoretical Chemistry*, *1008*, 52-60.

Chakravarthy, V. A., Sailaja, B., & Praveen Kumar, A. (2016). Method development and validation of ultraviolet-visible spectroscopic method for the estimation of hepatitis-c drugs-daclatasvir and sofosbuvir in active pharmaceutical ingredient form. *Asian. J. Pharm. Clin. Res*, *9*, 61-66.

Charlton, M., Everson, G. T., Flamm, S. L., Kumar, P., Landis, C., Brown Jr, R. S., ... & Romero-Marrero, C. (2015). Ledipasvir and sofosbuvir plus ribavirin for treatment of HCV infection in patients with advanced liver disease. *Gastroenterology*, *149*(3), 649-659.

Cheney, M. L., Weyna, D. R., Shan, N., Hanna, M., Wojtas, L., & Zaworotko, M. J. (2011). Coformer selection in pharmaceutical cocrystal development: a case study of a meloxicam aspirin cocrystal that exhibits enhanced solubility and pharmacokinetics. Journal of pharmaceutical sciences, 100(6), 2172-2181.

Childs, S. L., Chyall, L. J., Dunlap, J. T., Smolenskaya, V. N., Stahly, B. C., & Stahly, G. P. (2004). Crystal engineering approach to forming cocrystals of amine hydrochlorides with organic acids. Molecular complexes of fluoxetine hydrochloride with benzoic, succinic, and fumaric acids. Journal of the American Chemical Society, 126(41), 13335-13342.

Choi, J. S., & Park, J. S. (2017). Design of PVP/VA S-630 based tadalafil solid dispersion to enhance the dissolution rate. *European journal of pharmaceutical sciences*, *97*, 269-276.

Chun, N. H., Wang, I. C., Lee, M. J., Jung, Y. T., Lee, S., Kim, W. S., & Choi, G. J. (2013). Characteristics of indomethacin–saccharin (IMC–SAC) co-crystals prepared by an anti-solvent crystallization process. *European Journal of Pharmaceutics and Biopharmaceutics*, *85*(3), 854-861.

Costa, P., & Lobo, J. M. S. (2001). Modeling and comparison of dissolution profiles. *European journal of pharmaceutical sciences*, *13*(2), 123-133.

Cysewski, P., & Przybyłek, M. (2017). Selection of effective cocrystals former for dissolution rate improvement of active pharmaceutical ingredients based on lipoaffinity index. *European Journal of Pharmaceutical Sciences*, *107*, 87-96.

Dizaj, S. M., Mennati, A., Jafari, S., Khezri, K., & Adibkia, K. (2015). Antimicrobial activity of carbon-based nanoparticles. *Advanced pharmaceutical bulletin*, *5*(1), 19..

Essa, E. A., Elbasuony, A. R., Abdelaziz, A. E., & El Maghraby, G. M. (2019). Co-crystallization for enhanced dissolution rate of bicalutamide: preparation and evaluation of

rapidly disintegrating tablets. *Drug Development and Industrial Pharmacy*.

He, G., Jacob, C., Guo, L., Chow, P. S., & Tan, R. B. (2008). Screening for cocrystallization tendency: the role of intermolecular interactions. *The Journal of Physical Chemistry B*, *112*(32), 9890-9895.

Hu, L., Yang, J., Liu, W., & Li, L. (2011). Preparation and evaluation of ibuprofen-loaded microemulsion for improvement of oral bioavailability. *Drug Delivery*, *18*(1), 90-95.

Islam, M. A., Alam, M. M., Sikdar, K. Y. K., Al Hossain, A. M., & Rouf, A. S. S. (2021). Development and Characterization of a Combination Tablet Dosage Form Containing Sofosbuvir and Ribavirin Using Design of Experiments (DoE) Approach. *Dhaka University Journal of Pharmaceutical Sciences*, *20*(1), 121-133.

Jaafar, I. S., & Radhi, A. A. (2020). Preparation and physicochemical characterization of cocrystals for enhancing the dissolution rate of glimepiride. *Journal of Advanced Pharmacy Education & Research| Jul-Sep*, *10*(3), 69.

Jaipal, A., Pandey, M. M., Charde, S. Y., Raut, P. P., Prasanth, K. V., & Prasad, R. G. (2015). Effect of HPMC and mannitol on drug release and bioadhesion behavior of buccal discs of buspirone hydrochloride: In-vitro and in-vivo pharmacokinetic studies. *Saudi Pharmaceutical Journal*, *23*(3), 315-326.

Jones, W., Motherwell, W. S., & Trask, A. V. (2006). Pharmaceutical cocrystals: An emerging approach to physical property enhancement. *MRS bulletin*, *31*(11), 875-879..

Kang, J. H., Oh, D. H., Oh, Y. K., Yong, C. S., & Choi, H. G. (2012). Effects of solid carriers on the crystalline properties, dissolution and bioavailability of flurbiprofen in solid self-nanoemulsifying drug delivery system (solid SNEDDS). *European journal of pharmaceutics and biopharmaceutics*, *80*(2), 289-297.

Kassem, F. A., Abdelaziz, A. E., & El Maghraby, G. M. (2021). Ethanol-assisted kneading of apigenin with arginine for enhanced dissolution rate of apigenin: development of rapidly disintegrating tablets. *Pharmaceutical Development and Technology*, *26*(6), 693-700.

Khadka, P., Ro, J., Kim, H., Kim, I., Kim, J. T., Kim, H., ... & Lee, J. (2014). Pharmaceutical particle technologies: An approach to improve drug solubility, dissolution and bioavailability. *Asian journal of pharmaceutical sciences*, *9*(6), 304-316.

Khan, K. A. (1975). The concept of dissolution efficiency. *Journal of pharmacy and pharmacology*, *27*(1), 48-49.

Lankalapalli, S., Sandela, D., Pudi, A., & Kolluru, N. (2017). Preparation and evaluation of sofosbuvir polyelectrolyte microparticles. *International journal of Research in pharmacy and Chemistry*, *7*(4), 547-557..

Mehmood, Y., Khan, I. U., Shahzad, Y., Khan, R. U., Khalid, S. H., Yousaf, A. M., ... & Shah, S. U. (2020). Amino-decorated mesoporous silica nanoparticles for controlled sofosbuvir delivery. *European journal of pharmaceutical sciences*, *143*, 105184.184.

Moretti, M. D. L., Gavini, E., Juliano, C., Pirisino, G., & Giunchedi, P. (2001). Spray-dried microspheres containing ketoprofen formulated into capsules and tablets. *Journal of microencapsulation*, *18*(1), 111-121.

Ochi, M., Inoue, R., Yamauchi, Y., Yamada, S., & Onoue, S. (2013). Development of meloxicam salts with improved dissolution and pharmacokinetic behaviors in rats with impaired gastric motility. *Pharmaceutical research*, *30*(2), 377-386.

Ochi, M., Kawachi, T., Toita, E., Hashimoto, I., Yuminoki, K., Onoue, S., & Hashimoto, N. (2014). Development of nanocrystal formulation of meloxicam with improved dissolution and pharmacokinetic behaviors. *International journal of pharmaceutics*, *474*(1-2), 151-156.

Padrela, L., Rodrigues, M. A., Velaga, S. P., Fernandes, A. C., Matos, H. A., & de Azevedo, E. G. (2010). Screening for pharmaceutical cocrystals using the supercritical fluid enhanced atomization process. *The Journal of Supercritical Fluids*, *53*(1-3), 156-164.

Panzade, P., Shendarkar, G., Shaikh, S., & Rathi, P. B. (2017). Pharmaceutical cocrystal of piroxicam: design, formulation and evaluation. Advanced pharmaceutical bulletin, 7(3), 399.

Pêcego, I. G. (2018). *Synthesis of glibenclamide cocrystals through grinding methods* (Doctoral dissertation).

Rajbanshi, K., Bajracharya, R., Shrestha, A., & Thapa, P. (2014). Dissolution enhancement of aceclofenac tablet by solid dispersion

technique. *International Journal of Pharma Sciences and Research*, *5*(4), 127-139.

Rawat, S., & Jain, S. K. (2004). Solubility enhancement of celecoxib using β-cyclodextrin inclusion complexes. *European journal of pharmaceutics and biopharmaceutics*, *57*(2), 263-267.

Reis, C. P., Ferreira, J. P., Candeias, S., Fernandes, C., Martinho, N., Aniceto, N., ... & Figueiredo, I. V. (2014). Ibuprofen nanoparticles for oral delivery: proof of concept. *Journal of Nanomedicine & Biotherapeutic Discovery*, *4*(1), 1.

Samprasit, W., Akkaramongkolporn, P., Kaomongkolgit, R., & Opanasopit, P. (2018). Cyclodextrin-based oral dissolving films formulation of taste-masked meloxicam. *Pharmaceutical Development and Technology*, *23*(5), 530-539.

Sanphui, P., Kumar, S. S., & Nangia, A. (2012). Pharmaceutical cocrystals of niclosamide. Crystal growth & design, 12(9), 4588-4599.

Sironi, D., Rosenberg, J., Bauer-Brandl, A., & Brandl, M. (2017). Dynamic dissolution-/permeation-testing of nano-and microparticle formulations of fenofibrate. *European Journal of Pharmaceutical Sciences*, *96*, 20-27.

Sopyan, I., Fudholi, A., Muchtaridi, M., & Sari, I. P. (2017). Simvastatin-nicotinamide co-crystal: design, preparation and preliminary characterization. *Tropical Journal of Pharmaceutical Research*, *16*(2), 297-303.

Turker, M. (2013). FDA Approves 'Game Changer'Hepatitis-C Drug Sofosbuvir. *Medscape. 6th December*..

Velaga, S. P., Basavoju, S., & Boström, D. (2008). Norfloxacin saccharinate–saccharin dihydrate cocrystal–A new pharmaceutical cocrystal with an organic counter ion. *Journal of Molecular Structure*, *889*(1-3), 150-153.

Viertelhaus, M., & Hafner, A. (2015). Co-crystals and their advantages for APIs with challenging properties. *CHIMICA OGGI-CHEMISTRY TODAY*, *33*(5), 23-26.

Wang, I. C., Lee, M. J., Sim, S. J., Kim, W. S., Chun, N. H., & Choi, G. J. (2013). Anti-solvent co-crystallization of carbamazepine and saccharin. *International journal of pharmaceutics*, *450*(1-2), 311-322.

Xing, Q., Song, J., You, X., Xu, D., Wang, K., Song, J., ... & Hu, H. (2016). Microemulsions containing long-chain oil ethyl oleate improve the oral bioavailability of piroxicam by increasing drug solubility and lymphatic transportation simultaneously. *International journal of pharmaceutics*, *511*(2), 709-718.

Ziaee, A., Albadarin, A. B., Padrela, L., Faucher, A., O'Reilly, E., & Walker, G. (2017). Spray drying ternary amorphous solid dispersions of ibuprofen–An investigation into critical formulation and processing parameters. *European Journal of Pharmaceutics and Biopharmaceutics*, *120*, 43-51.